J Mater Sci (2014) 49:463–480
DOI 10.1007/s10853-013-7705-y

REVIEW

A review: carbon nanofibers from electrospun polyacrylonitrile and their applications

Lifeng Zhang · Alex Aboagye · Ajit Kelkar · Chuilin Lai · Hao Fong

Received: 17 June 2013 / Accepted: 26 August 2013 / Published online: 14 September 2013
© Springer Science+Business Media New York 2013

Abstract Carbon nanofibers with diameters that fall into submicron and nanometer range have attracted growing attention in recent years due to their superior chemical, electrical, and mechanical properties in combination with their unique 1D nanostructures. Unlike catalytic synthesis, electrospinning polyacrylonitrile (PAN) followed by stabilization and carbonization has become a straightforward and convenient route to make continuous carbon nanofibers. This paper is a comprehensive and state-of-the-art review of the latest advances made in development and application of electrospun PAN-based carbon nanofibers. Our goal is to demonstrate an objective and overall picture of current research work on both functional carbon nanofibers and high-strength carbon nanofibers from the viewpoint of a materials scientist. Strategies to make a variety of carbon nanofibrous materials for energy conversion and storage, catalysis, sensor, adsorption/separation, and biomedical applications as well as attempts to achieve high-strength carbon nanofibers are addressed.

Background

Carbon fibers are of great technological and industrial importance because of their comprehensive properties such as very high strength to weight ratio, excellent chemical resistance, and superior electrical and thermal conductivity [1, 2]. They have been particularly used to develop high-performance fiber-reinforced composites which are highly desirable in automotive, aerospace, and sport industries. Activated carbon fibers (ACFs) fall into another category of carbon fibers that bear high specific surface area resulting from pore-creating surface modification. ACFs have found their applications in gas adsorption/storage and water treatment [3, 4].

There are generally two approaches to produce carbon fibers: vapor growth and spinning. Synthesis of carbon fibers from vapor growth was explored in 1970s and 1980s [5, 6]. Carbon fibers were obtained through catalytic decomposition of certain hydrocarbons in the presence of metal particles (catalysts) but encountered great difficulties in mass-production. Spinning thus became the most commonly used approach that comprises spinning of polymeric precursor fibers and following thermal treatment. Although any material with carbon back-bone can be used as precursor of carbon, carbon fibers are normally produced from three polymeric precursors: polyacrylonitrile (PAN), cellulose, and pitch. Among these three precursors, PAN has received major attention due to its high carbon yield and superior mechanical properties of the resultant carbon fibers. PAN is actually the precursor for about 90 % of carbon fibers manufactured today [7]. It is noteworthy that carbon fibers with the highest mechanical strength have been produced exclusively from PAN copolymer precursors containing 0.5–8 wt% co-monomers such as acids (e.g., itaconic acid), vinyl esters (e.g., methyl methacrylate), and others [2]. The inclusion of co-monomers partially disrupts nitrile–nitrile interactions in PAN macromolecules, rendering the copolymer more readily soluble in spinning solvents, allowing better macromolecular chain orientation

L. Zhang (✉) · A. Aboagye · A. Kelkar
Joint School of Nanoscience and Nanoengineering,
North Carolina Agricultural and Technical State University,
Greensboro, NC 27401, USA
e-mail: lzhang@ncat.edu

C. Lai · H. Fong (✉)
Department of Chemistry and Applied Biological Sciences,
South Dakota School of Mines and Technology,
Rapid City, SD 57701, USA
e-mail: Hao.Fong@sdsmt.edu

in precursor fibers, and making stabilized and carbonized fibers more structurally homogeneous. In this review, no difference is treated between PAN homopolymer and copolymer and the name of PAN is generally used for both.

Conventional spinning of PAN is mostly done by wet spinning and dry-jet wet spinning although dry spinning and even melt spinning are also achievable [1]. In wet spinning, a spinneret with 40–80 μm diameter orifices is immersed in a coagulation bath and a spin dope (PAN solution) is extruded directly into the coagulation bath to form jets/filaments. In dry-jet wet spinning, a spinneret is positioned a few millimeters above a coagulation bath and jets/filaments are extruded vertically into the bath. The dry-jet wet spun fibers exhibit finer linear density and higher strength and thus become more popular. To make carbon fibers, PAN precursor fibers are first stabilized under tension through a controlled heating procedure normally in air between 200 and 300 °C to convert PAN to a ladder compound, which enables these fibers to undergo further processing at higher temperature. Stabilized precursor fibers are subsequently converted to carbon fibers in the process of carbonization that involves heat treatment in an inert atmosphere up to 1500 °C. In this process, almost all elements other than carbon are eliminated in the form of appropriate byproducts and a graphite-like structure is formed. The carbon fibers that are produced from above-mentioned wet or dry-jet wet spinning typically have diameters ranging from a few to a couple tens of micrometers.

With widespread interest in nanomaterials recently, making carbon fibers with diameters fall into submicron and nanometer range (termed as carbon nanofibers) has attracted growing attention. The production of carbon nanofibers falls into the same two categories as their conventional counterpart: vapor growth and spinning. The approach of vapor phase growth, i.e., catalytic synthesis, has been investigated [8–10] and graphitic carbon nanofibers (GCNFs) are grown from carbon-containing gases by using metallic catalysts. Nonetheless, these carbon nanofibers are relatively short and difficult to be aligned, assembled, and processed into applications, not to mention their low product yield, expensive manufacturing equipment, and significant amount of catalyst residue. The rapidly developing technique of "electrospinning," on the contrary, provides a straightforward way to make continuous carbon fibers at sub-micrometer scale (typically 100–1000 nm), approximately two to three orders of magnitude smaller than their conventional counterpart [11–14]. Similar as conventional carbon fiber production, PAN is the most often used precursor polymer for carbon nanofibers from electrospinning. There are a couple of recent published reviews that partially covered the topic of carbon nanofibers from electrospun PAN and presented especially the researches before 2010 [13, 14]. Due to the rapid upsurge in research activities devoted to carbon nanofibers from electrospun PAN, herein we aim to a comprehensive and state-of-the-art review on development and application of electrospun PAN-based carbon nanofibers from the point of view of a nanomaterials scientist with an opening introduction to electrospinning of PAN and technical strategy to make carbon nanofibers therefrom. This manuscript covers the basic aspects of the electrospun PAN-based carbon nanofibers as well as their practical applications and reveals a complete picture of the research work in this field in the past 3 years.

PAN-based carbon nanofibers from electrospinning

Electrospinning of PAN

During the last decade, extensive researches have been conducted on electrospinning of PAN [15–18]. Unlike conventional fiber spinning techniques such as dry-spinning, wet-spinning or melt-spinning, electrospinning of PAN is driven by electrical force instead of mechanical force and follows a different thinning mechanism.

When exposed to an electric field, the droplet of PAN solution at the tip of spinneret deforms from the shape caused by surface tension alone and forms Taylor cone [19]. As the applied electrical potential reaches a critical value and the resulting electrical force on the droplet of PAN solution overcomes its surface tension and viscoelastic force, a jet of PAN solution ejects from the tip of Taylor cone and electrospinning begins. The jet then follows a bending, winding, and spiraling path in 3D and becomes thinner with the increase of loop circumference, as shown in Fig. 1. This phenomenon is termed as "bending (or whipping) instability" [20–23], the dominant thinning mechanism in electrospinning. Typically the bending instability causes the length of an electrospinning jet to elongate by more than 10,000 times in a very short time period (50 ms or less) with concurrent fiber thinning. Thus, the elongation or drawing rate during the bending instability is extremely large (up to 1,000,000 s^{-1} [21]). Such enormous drawing rate, which is not accessible from other methods, can effectively stretch PAN macromolecular chains in nanofibers and closely align them along nanofiber axes [24]. In addition to fast evaporation of solvent, i.e., over 99 % solvent in electrospinning jets can be removed during or shortly after bending instability, the macromolecular orientation in electrospun PAN nanofibers is likely to retain. Nonetheless, the chaotic trajectory of electrospinning jets makes electrospun PAN nanofibers very difficult to form ordered and/or aligned assemblies

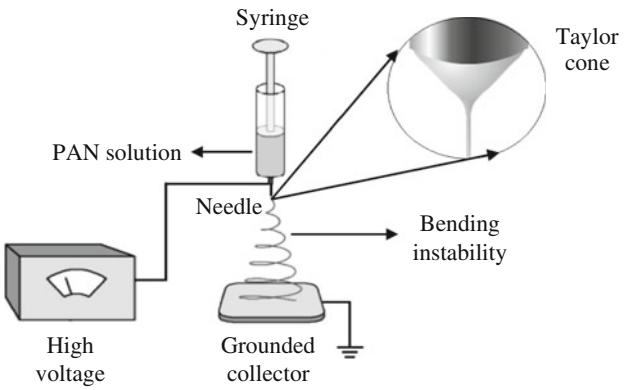

Fig. 1 Schematic diagram of electrospinning PAN including basic electrospinning setup, Taylor cone, and bending instability

and intrinsically resulted in nonwoven mats that are composed of randomly deposited PAN nanofibers.

Due to the concomitant high specific surface area, electrospun PAN mats (also termed as felts, membranes, or other equivalent names) have seen extensive uses in the fields of adsorption/filtration/separation [25, 26] and catalysis [27, 28].

Carbonization of electrospun PAN nanofibers

Similar to production of conventional carbon fibers, carbon nanofibers have been successfully prepared by electrospinning PAN followed by a two-step process: stabilization and carbonization. Varied stabilization and carbonization conditions have been reported for electrospun PAN nanofibers in which stabilization was carried out in air at temperatures between 200 and 300 °C while carbonization was further conducted in inert atmosphere up to 2800 °C [29–34]. In order to reduce mass loss and dimension shrinkage, progressive and multi-stage heating procedures were developed to cover stabilization and carbonization (Fig. 2). The progressive stabilization and carbonization procedure of 5 °C/min from 30 to 230 °C, 1 °C/min from 230 to 270 °C, then 5 °C/min from 270 to 800 °C led to little change in fiber packing, much less planar dimensional shrinkage, and significant increase of carbon yield [35] compared to the reported procedure in which stabilization was carried out at 200 °C for 30 min followed by carbonization at 750 °C for 1 h [30].

Overview of research on carbon nanofibers from electrospun PAN

Unlike their conventional counterpart, single carbon nanofibers from electrospun PAN exhibit weak strength in spite of their potential to become high-strength fibers considering their smaller sizes and the drawing feature in electrospinning process. This is because PAN macromolecular chains in electrospun nanofibers, especially in the presence of some trace amount of solvent, may relax to some extent after depositing on collector and lose their formerly drawing-lead orientation. It is well known that many structural imperfections in the precursor fibers are likely to be retained in the resulting carbon fibers [36]. The loss of macromolecular orientation in final electrospun PAN nanofibers may be the reason that causes inferior mechanical properties of the resulting carbon nanofibers. In addition, when stress is applied to a carbon nanofiber nonwoven mat, only a small amount of nanofibers share tensile stress inside the nonwoven mat due to their random deposit and stack feature and these nanofibers are easily separated from each other at junction points under stress. Therefore the mechanical strength of either individual carbon nanofibers or their nonwoven mats is inevitably weak [32]. Up to date carbon nanofibers from electrospun PAN are mostly restricted to those applications that do not rely on mechanical properties but on their superior physical properties such as high specific surface area, great electrical conductivity, and good biocompatibility. This type of carbon nanofibers is referred to as functional carbon nanofibers. The research in developing strong carbon nanofibers from electrospun PAN, however, does not fade out. Instead it is becoming a point of interest due to the potential to overcome current technological obstacles and further improve mechanical strength of carbon fibers [36]. This type of carbon nanofibers is referred to as

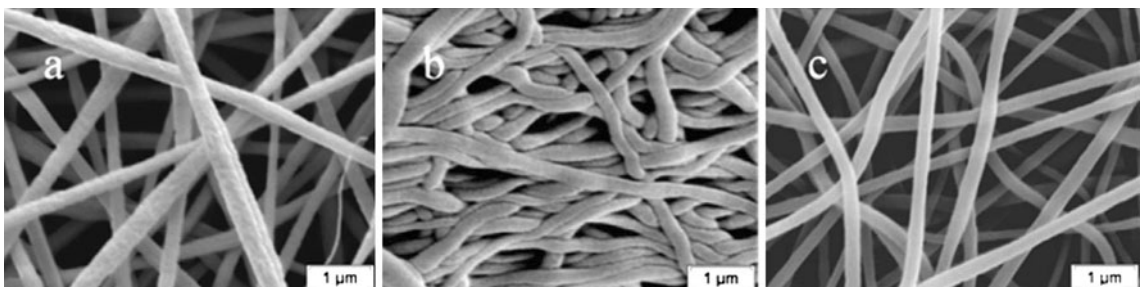

Fig. 2 Representative SEM images of electrospun PAN nanofibers from 8 % PAN solution in *N*,*N*-dimethylformamide (DMF) (**a**); carbon nanofibers derived from **a** with a two-step heating: 200 °C for 30 min and 750 °C for 1 h (**b**); carbon nanofibers derived from **a** with a multi-step progressive heating: 5 °C/min from 30 to 230 °C, 1 °C/min from 230 to 270 °C, then 5 °C/min from 270 to 800 °C (**c**) [35]

high-strength carbon nanofibers. In the following part, the above-mentioned two types of carbon nanofibers are addressed respectively.

PAN-based functional carbon nanofibers and their applications

Energy conversion and storage

Innovative energy conversion and storage systems, e.g., rechargeable lithium-ion batteries (LIBs), supercapacitors, and fuel cells, are urgently demanded to meet the increasing energy needs of modern society to fulfill the newly emerging applications such as portable electronics, electric vehicles, and industrial power management [37]. The performance of these devices depends dominantly on the properties of their electrode materials. Carbon nanotubes have been extensively used as additive for both anode and cathode materials in energy conversion and storage systems [38, 39] because they possess not only common advantages of carbon materials such as good chemical stability, thermal stability, and electrical conductivity, but also high specific surface area and better charge transport properties. However, carbon nanotubes often require delicate purification process to remove residue metal catalyst, which may have significant adverse effect on their electrochemical performance. Compare to carbon nanotubes, carbon nanofibers from electrospun PAN have similar advantages as 1D carbon nanostructure and furthermore they are inexpensive, continuous, and relatively easy to be applied into applications. The adjustable electrical properties of carbon nanofibers from electrospun PAN have been evaluated and confirmed [40], which demonstrated their potentials as efficient electrode materials.

An additional merit of carbon nanofiber mat from electrospun PAN is its ease of handling that is resulted from the interconnected nanofiber network structure. This allows the elimination of polymer binders and conductive fillers in electrodes for better results. Nonetheless, the original carbon nanofiber mats from electrospun PAN could not resolve all limitations that their conventional counterparts face. In most recent years, researches of carbon nanofibers from electrospun PAN have been directed to even higher specific surface area and multiple-phase nanostructures to address a comprehensive improvement on electrochemical performance.

Lithium-ion batteries (LIBs)

LIBs are attractive power sources for a wide range of electric devices from cell phones and laptop computers to hybrid electric vehicles. Although stand-alone carbon nanofibers from electrospun PAN have been demonstrated as a good anode material for LIBs [41], there have been tremendous interests in developing novel carbon nanomaterials for advanced LIB electrodes to improve overall energy capacity and cycling stability.

Adding second component into PAN spin dopes may either improve PAN carbonization or acquire porous nanostructures upon second component removal. A novel type of carbon nanofibers was derived from electrospinning PAN with a conductive polymer, polypyrrole (PPy), in *N*,*N*-dimethylformamide (DMF) solvent [42]. Some intermolecular interactions between PAN and PPy phases were observed in the bicomponent precursor nanofibers, which influenced the stabilization and carbonization of PAN. The carbon nanofibers derived therefrom at 700 °C were used as anodes for LIB without adding any polymer binder or conductive material. Improved overall electrochemical performance was observed compared to the present electrode material in commercial LIBs. Hollow graphitic carbon nanospheres were introduced into PAN-based amorphous carbon nanofibers through the combination of electrospinning, calcination, and acid treatment [43]. The hollow graphitic carbon nanospheres provided extra sites for lithium-ion storage and served as buffers for withstanding large volume expansion and shrinkage during lithium-ion intercalation process. The diffusion of lithium ions as well as the collection and transport of electrons during the cycling process were simultaneously improved.

Various carbon composite nanofibers have been developed lately because carbon composite nanofibers can combine long cycle life from carbon and high storage capacity from the second component. For example, silicon nanoparticles were directly integrated into carbon nanofibers through electrospinning PAN spin dopes containing Si nanoparticles followed by stabilization and carbonization [44]. More importantly, integration of metal salts as precursors of metal or metal oxide in PAN spin dopes has led to a variety of carbon/metal or carbon/metal oxide composite nanofibers.

Tin (Sn) and tin oxide (SnO_2) have been considered as promising anode materials for LIBs due to their much higher specific capacities than the commercial graphite. However, Sn-based materials suffer from poor cycling performance due to large volume change resulting from repeated lithium insertion and extraction [45]. Carbon/Sn composite nanofibers were fabricated from electrospinning PAN solution containing $SnCl_4$ followed by a regular stabilization and carbonization at varied temperatures [46]. The resultant carbon/Sn nanofiber anode exhibited large reversible capacity and relatively good cycling performance in LIB. In another research, carbon/SnO_2 composite nanofibers were synthesized by adding tin sulfate ($SnSO_4$) to PAN nanofibers either through electrospinning (I) or after electrospinning (II) followed by heat treatment and

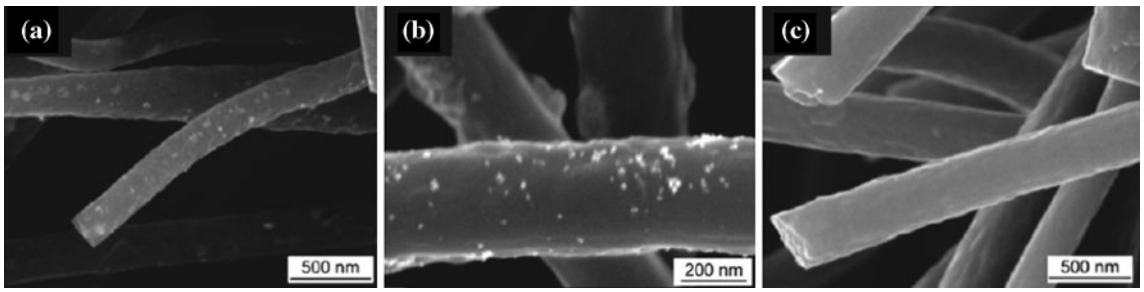

Fig. 3 SEM images of carbon/SnO_2 composite nanofibers from electrospinning PAN solution followed by soak in aqueous $SnSO_4$ solution and subsequent carbonization (**a**, **b**) and carbon nanofibers from electrospinning PAN solution followed by soak in water and subsequent carbonization (**c**) [47]

used as anode in LIB [47]. In approach I, $SnSO_4$ was directly incorporated in PAN solution for electrospinning; in approach II, $SnSO_4$ was solution-coated on PAN nanofiber surface prior to final thermal treatment. The approach II yielded a greater concentration of tin (Fig. 3). These carbon/SnO_2 nanofibers showed greater discharge capacity than pure carbon nanofibers when they were evaluated as anode for LIB half-cell. The carbon/SnO_2 nanofibers complemented the long cycle life of carbon with the high lithium storage capacity of SnO_2. The high surface-to-volume ratio of nanofibers improved the accessibility for lithium intercalation as compared to graphite-based anodes and simultaneously eliminated the need for binders or conductive additives. Despite the above-mentioned advantages, thermal reduction of SnO_2 to metallic Sn is unavoidable in the process of carbonization of PAN nanofibers containing tin salt, leading to the formation of large Sn agglomerate that in turn induce capacity fading during the charge/discharge cycles. A recent research revealed that adding a small amount of Ni in the PAN spin dope could improve SnO_2's thermal stability and prevent formation of large Sn agglomerate in the final SnO_2/carbon composites nanofibers [48].

Carbon/Ni composite nanofibers were acquired through electrospinning nickel acetate/PAN solutions followed by carbonization [49]. The evaluation result for LIB performance suggested that the content of Ni in the composite nanofibers had a huge influence on final electrochemical performance. Compared to pure carbon nanofiber electrode, carbon/Ni composite nanofibers containing 12 wt% Ni exhibited high reversible capacity, enhanced cyclic retention, and excellent rate capability when used as binder-free anode for LIBs. The improvement of electrochemical performance is attributed to the synergistic effect of Ni nanoparticles and carbon matrix as well as the unique 1D nanofiber structure with large surface area and high length/diameter ratio. Similar results were reported by using nickel nitrate as Ni precursor [50].

Carbon/TiO_2 composite nanofibers were prepared by electrospinning PAN solution containing TiO_2 precursor (titanium (IV) isopropoxide) followed by thermal pyrolysis and oxidization and evaluated as anode material for LIB [51]. The composite nanofibers demonstrated excellent electrochemical performance due to the structure of encapsulated TiO_2 nanocrystal in porous carbon matrix. Similarly including ferric chloride and manganese acetate in PAN spin dopes resulted in Fe_2O_3 and MnO/Mn_3O_4 nanoparticle-loaded carbon nanofibers, respectively, which has been used as anode material to improve performance of LIBs [52, 53].

In addition to be used as anode material, carbon composite nanofibers have also been employed as cathode materials for LIBs. Li_2MnSiO_4 has been considered as a promising cathode material with an extremely high theoretically capacity. However, it has intrinsic low conductivity and poor structural stability. To realize its high capacity and improve cycling performance, Cr and Fe doping were coupled with PAN electrospinning to make $Li_2Mn_{(1-x)}Cr_xSiO_4$/carbon and $Li_2Mn_{0.8}Fe_{0.2}SiO_4$/carbon composite nanofibers [54, 55]. The composite nanofibers exhibited a high discharge capacity and stable cycling performance. $LiFePO_4$ is recently developed as alternative positive electrode for LIBs. To improve electrical conductivity and lithium-ion diffusivity, $LiFePO_4$/carbon/carbon black composite nanofibers were prepared from a simple sol–gel process on the surface of electrospun PAN/carbon black-based carbon nanofibers in a solution containing lithium, iron, and phosphate ions and showed good electrochemical performance as cathode material for LIB [56]. In another research, carbon/$LiFePO_4$/graphene composite nanofibers were acquired by electrospinning mixed DMF solution of PAN, $LiFePO_4$ precursor and graphene followed by sol–gel techniques and heat treatment [57]. It was observed that cells containing carbon/$LiFePO_4$/graphene composite nanofiber cathode demonstrated good electrochemical performance in terms of capacity, cycle life, and rate capability. Carbon/LiF/Fe composite nanofibers were obtained from electrospinning of LiF/ferrocene/PAN precursor solution followed by heat treatment and evaluated as a cathode material for LIBs [58]. LiF/Fe/carbon composite nanofibers prepared from a 21 wt%

precursor solution showed the most uniform structure with evenly distributed LiF/Fe nanoparticles throughout the carbon nanofiber matrix. The more homogeneous distribution of LiF/Fe particles in the carbon nanofiber matrix, the better electrochemical performance was observed.

Supercapacitors

Electric double layer capacitors (EDLCs), also known as supercapacitors, have received growing attention because they can achieve a higher energy density than conventional capacitors and provide a better power density than batteries. Porous carbon nanofibers showed their advantage in making high capacity supercapacitors because of their even higher specific surface area. Various forms and textures of porous carbons have been investigated as possible electrode materials for surpercapacitors.

A common method to make porous carbon nanofibers is to integrate other components with PAN in spin dopes followed by electrospinning, stabilization, and carbonization. It was found that the presence of Si-containing compounds such as phenylsilane (PS) [59], tetraethyl orthosilicate (TEOS) [60], and polymethylhydrosiloxane (PMHS) [61] in PAN nanofibers created micropores on the outer surface of corresponding carbon nanofibers in the process of carbonization, which resulted in highly microporous carbon nanofibers with ultra-high specific surface area up to 1200 m^2/g. As electrode materials for supercapacitor applications, these carbon nanofibers demonstrated much higher specific capacitance and energy/power density values than the original carbon nanofibers derived from PAN alone. Composite carbon nanofibers containing vanadium pentoxide (V_2O_5) were prepared from electrospinning PAN-DMF solution containing synthesized V_2O_5 nanotubular structures [62]. It is revealed that the content of V_2O_5 was the major factor that was responsible for the morphology and pore structures. The electrode made of these C/V_2O_5 composite nanofibers led to the highest specific capacitance of 150 F/g and energy density of 18.8 W h kg^{-1} over a power density range of 400–20,000 W kg^{-1}. In another report, boric acid (H_3BO_3) and urea were included in PAN electrospinning solution to introduce boron and nitrogen functional groups in carbon nanofibers and to increase total higher surface area [63]. The electrode with these characteristics demonstrated better supercapacitor performances with specific capacitance of 180 F/g and energy density of 17.2–23.5 W h kg^{-1} in the power density range of 400–10,000 W kg^{-1}.

An innovative porous electrode material based on continuous graphene-embedded carbon nanofibers was used for supercapacitor applications (Fig. 4) [64]. The material was prepared by electrospinning PAN-DMF solution with oxidized graphene nanosheets followed by carbonization at 800 °C. Electrochemical measurements of this type of supercapacitor revealed the maximum specific capacitance of 263.7 F/g in 6 M KOH aqueous electrolyte. The supercapacitor also exhibited good cycling stability of energy storage with retention ratio of 86.9 % after 2000 cycles. Similar graphene-integrated carbon nanofibers were prepared by dispersing graphene in PAN/poly(methyl methacrylate) (PMMA) [65] or PAN/TEOS [66] solutions in DMF followed by electrospinning, stabilization, and subsequent carbonization with or without activation. PMMA, TEOS, and graphene functioned as pore-creating materials via thermal decomposition. Hierarchical pore structures with ultramicropores and mesopores were introduced. The supercapacitors made with these porous carbon nanofibers exhibited specific capacitance up to 150 F/g and energy density up to 75 W h kg^{-1}, respectively, while the corresponding values were only 60 F/g and 6 W h kg^{-1} from the supercapacitor made with carbon nanofibers from PAN alone.

A side-by-side electrospinning design was employed to make PAN/polyvinylpyrrolidone (PVP) side-by-side bicomponent nanofibers (Fig. 5 top) which were used for interbonded carbon nanofiber membranes to increase charge-transfer efficiency in electrochemistry-associated processes [67]. The fiber–fiber interconnections in final carbon nanofiber membranes were simply established by a multiple-step pyrolysis, i.e., room temperature to 300 °C (2 h in air flow), 300–500 °C (2 h in N_2), and 500–970 °C (1 h in N_2), on PAN/PVP side-by-side precursor fibers that originally showed no inter-fiber connections. The inter-bonded fiber morphology was determined by the weight ratio of two polymer components in fibers (Fig. 5 bottom). The well interbonded carbon nanofiber membranes demonstrated larger electrochemical capacitances compared to those prepared from regular PAN/PVP polymer blend.

Higher PAN crystallinity in precursor fibers has been reported to be unfavorable to the cyclization step during PAN stabilization and results in a less uniform microstructure. To reduce PAN crystallinity and improve cyclization reaction of PAN, 9 % vinylimidazole was introduced to PAN molecules through co-polymerization. Poly (acrylonitrile-co-vinylimidazole) (poly(AN-co-VIM)) was synthesized, electrospun to nanofibers, and stabilized and carbonized subsequently [68]. The obtained carbon nanofiber mats were further activated and consequently reached a high surface area of 1120 m^2/g. These nanofiber mats were employed as electrode for coin cell supercapacitors and presented specific capacitances up to 122 F/g, and maximum energy and power densities of 47.4 Wh/kg and 7.2 kW/kg, respectively.

Dye-sensitized solar cells

Dye-sensitized solar cells (DSCs) have attracted extensive attention as low-cost alternative to Si solar cells. A typical

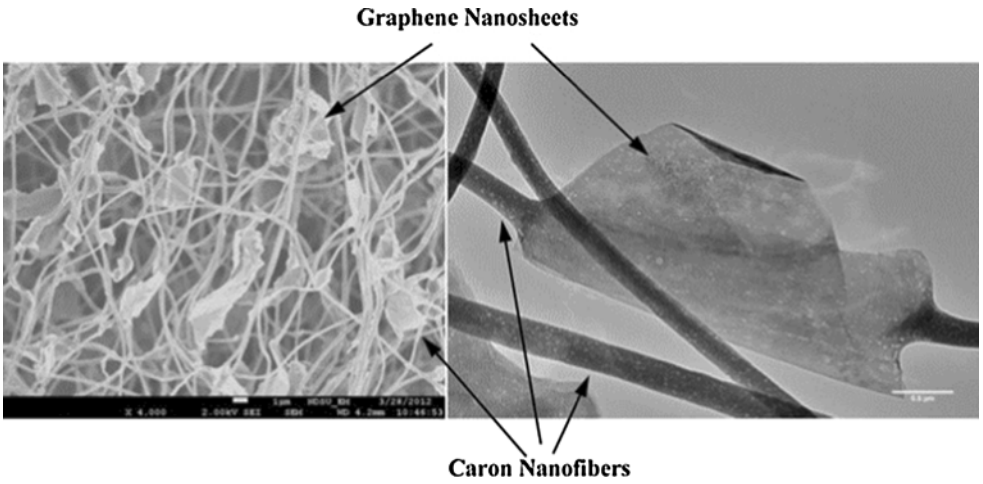

Fig. 4 SEM (*left*) and TEM (*right*) image of electrospun PAN-based carbon nanofibers that integrated with graphene nanosheet [64]

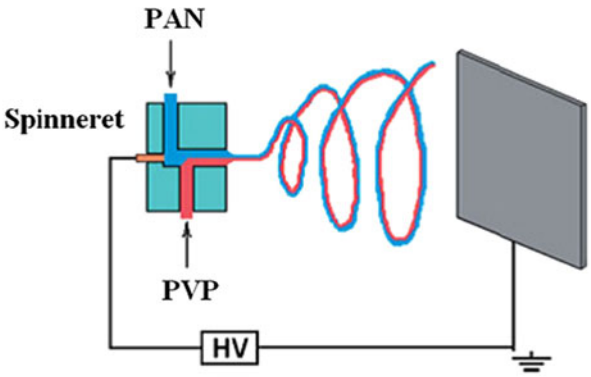

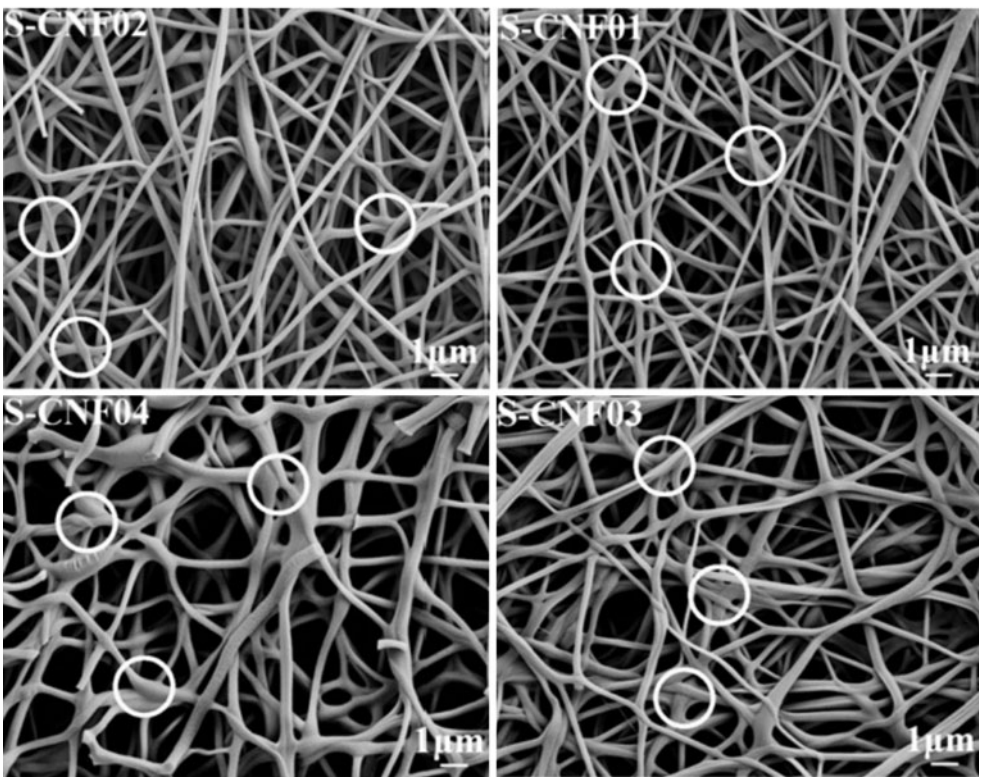

Fig. 5 Schematic diagram of the electrospinning setup to make PVP/PAN side-by-side precursor fibers (*top*) and SEM images of the inter-bonded carbon nanofiber membranes derived from water-treated PVP/PAN side-by-side precursor nanofibers with PVP/PAN weight ratios of 33/67 (S-CNF01), 43/57 (S-CNF02), 68/32 (S-CNF03), and 87/13 (S-CNF04) [67]

DSC consists of a photoanode and a counter electrode separated by an electrolyte containing an iodide/triiodide (I^-/I_3^-) redox couple. Platinum (Pt) counter electrodes have been widely used in DSCs because Pt is an efficient electrocatalyst for I_3^- reduction [69]. Nonetheless, Pt's high cost and corrosion by the redox species in the electrolyte directed research activities toward low-cost alternative counter electrode materials.

Carbon materials are abundant and possess high resistivity against corrosion. 1D and 2D carbon nanomaterials, i.e., carbon nanotubes and graphene nanosheets, respectively, have shown significant improvement in catalytic activity and power conversion efficiency in DSCs and demonstrated feasibility to replace Pt counter electrodes [70]. As another type of 1D carbon nanomaterial, carbon nanofibers from electrospun PAN were prepared and used as a low-cost alternative to Pt counter electrodes in DSCs (Fig. 6) [71]. Electrochemical measurements revealed that the counter electrode made with carbon nanofibers from electrospun PAN exhibited large surface area, low charge-transfer resistance, and fast reaction rates of I_3^- reduction, indicating that carbon nanofibers from electrospun PAN are an efficient electrocatalyst for the application in DSCs. In the following report, counter electrode made of Pt/carbon composite nanofibers (Pt/CNFs) was developed via solution-depositing Pt nanoparticles onto carbon nanofiber mats from electrospun PAN [72]. This type of electrode reduced the overall series resistance (R_{se}), decreased dark saturation current density (J_0), and increased shunt resistance (R_{sh}) of the DSCs. Correspondingly the Pt/CNFs-based DSCs achieved an energy conversion efficiency of $\sim$8 %, which was improved over those of pure Pt- or pure CNFs-based DSCs.

In another research, multi-walled carbon nanotube (MWCNT)-embedded mesoporous carbon nanofibers were prepared through a series of steps including electrospinning a 10 wt% PAN-DMF solution that contained 3 wt% MWCNT and 30 wt% SiO_2 nanoparticles followed by consecutive stabilization at 280 °C, carbonization at 800 °C, SiO_2 nanoparticle etching in 2 M NaOH aqueous solution, and activation in steam (Fig. 7) [73]. The cell using the prepared MWCNT-embedded mesoporous carbon nanofibers as counter electrode material exhibited even higher overall energy conversion efficiency than that of the cell using Pt counter electrode material.

Catalysis

Because of the ultra-high specific surface area, high chemical resistance, excellent electrical properties, and acceptable mechanical properties, carbon nanofibers from electrospun PAN are materials of choice for catalysis support. For example, carbon nanofibers from electrospun PAN were developed as electrode support for redox enzymes immobilization which applied to bioelectrocatalytic O_2 reduction [74]. The beneficial effects of these carbon nanofibers on electrical performance of the electrode were ascribed to high loading of active enzymes and fast kinetics at electrode surface. This type of material can be a promising candidate as enzymatic cathodes in biofuel cell devices.

To further increase the specific surface area of carbon nanofibers from electrospun PAN, consecutive stabilization, carbonization, and activation were performed to introduce porous structure [75]. The final activation of carbonized fibers was carried out in 30 vol% steam in nitrogen for 30 min at 800 °C. Without any other catalyst, the porous carbon nanofibers exhibited high activities for NO removal at room temperature due to their high surface area and more nitrogen species on surface. Carbon acted both as catalyst and adsorbent that facilitated the catalytic oxidation of NO into NO_2 or reduction of NO into N_2 with surface nitrogen pieces. In a following research, porous carbon nanofibers from electrospun PAN were further graphitized at 1900 and 2400 °C [76]. The results indicated that porous graphitic structure can improve the catalytic oxidation of NO dramatically at room temperature.

Pt-based electrocatalyst has been widely used at cathode of fuel cell because of their exceptional activity for oxygen reduction reaction (ORR). Research endeavors are taken nowadays for economic alternatives. Nitrogen-doped ultrathin carbon nanofibers (NCNFs) were developed by heating electrospun PAN nanofibers in NH_3 atmosphere and used to catalyze ORR in fuel cells [77]. Many graphitic layers were found to protrude from fiber surface with their edges exposed. The NCNFs demonstrated high electrocatalytic activity, long-term stability, and excellent tolerance to crossover effects for ORR at cathode of fuel cells. This material is a replacement of expensive Pt-based electrocatalyst for its low cost and high efficiency as cathodic catalyst for fuel cells. The cause of the high electrocatalytic activity was ascribed to pyrrolic-N on surface, exposed graphitic layer edges, and small diameters of the resultant NCNFs. In order to improve the catalysis activity for ORR in acid media, carbon nanofibers with unique porous morphology and hollow onion-like graphitic structure were produced by integrating FeC_2O_4 as iron source in PAN spinning solution followed by heat treatment in NH_3 atmosphere [78]. The prepared carbon nanofiber electrocatalyst containing Fe and N showed excellent catalytic activity and higher durability during ORR compared with commercial Pt-based catalyst. In another research, iron and cobalt-incorporated carbon nanofibers (FeCo-CNFs) were prepared as a substitute of Pt-based electrocatalyst via electrospinning of PAN solution containing iron (III) acetylacetonate and cobalt (II) acetylacetonate and subsequent

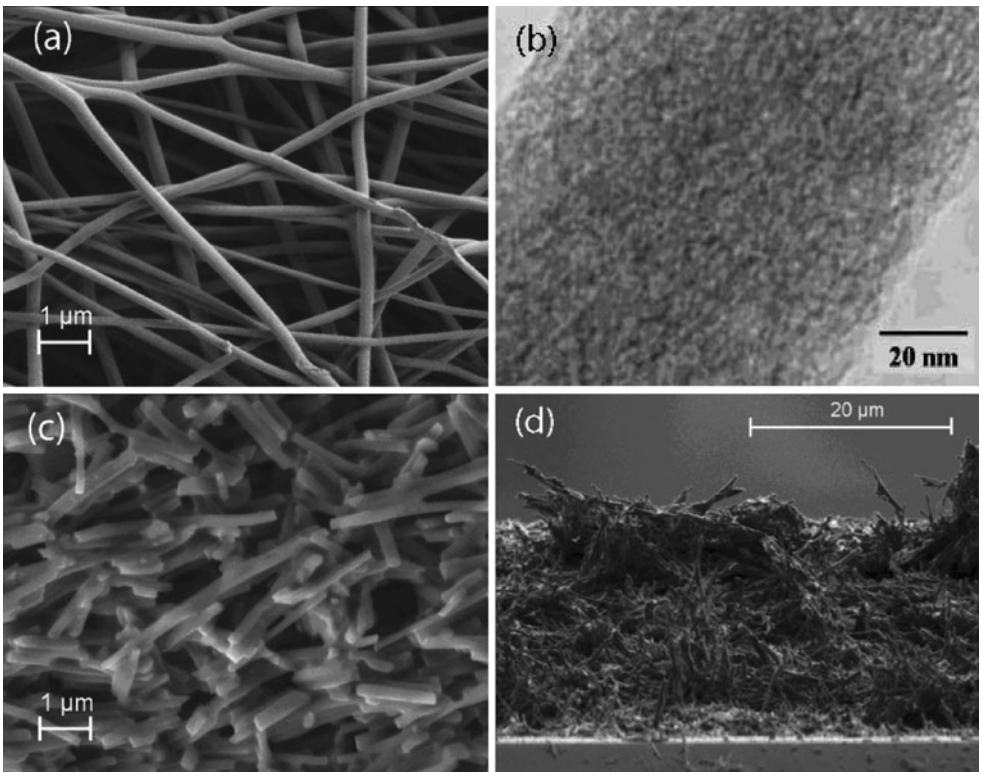

Fig. 6 **a** SEM image of the carbon nanofibers from electrospun PAN (CNFs); **b** TEM image of a typical single CNF; **c** top-view and **d** cross-section of CNFs-based counter electrode deposited by doctor blading on a FTO-glass substrate [71]

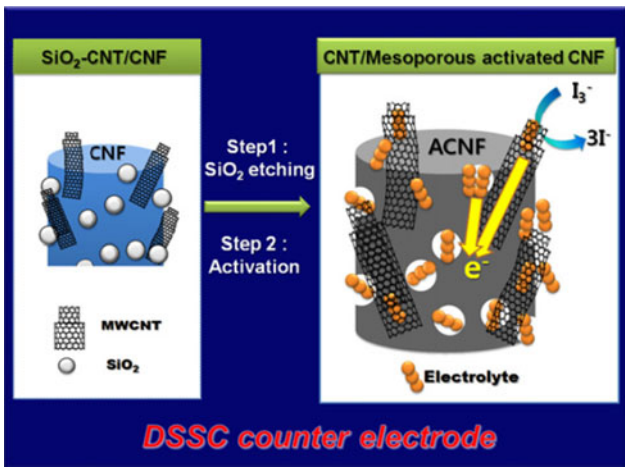

Fig. 7 The schematic diagram showing procedures to fabricate MWCNT-embedded mesoporous carbon nanofibers for counter electrode of DSCs [73]

pyrolysis of the blend precursor fibers [79]. The FeCo-CNFs demonstrated potential to replace expensive Pt-based catalysts for ORR in alkaline fuel cells due to comparable electrocatalytic activity, durability, and better ethanol tolerance in alcohol liquid fuel cells. The embedded Fe and Co nanoparticles would facilitate the formation of active sites comprised of nitrogen and oxygen rather than directly participating in ORR.

Microbial fuel cell (MFC) is a bio-electrochemical system that utilizes microorganisms to consume organic substrates at anodes and generate electricity. An important strategy to increase the bioelectrocatalytic performance of MFC is to develop biocompatible electrode materials with high surface area and long-term stability that can facilitate the maximum growth of bacteria and enhance electron transfer rate. Carbon nanofibers obtained from electrospun PAN and PAN blends with either activated carbon or graphite were tested as anodes in MFC [80]. The chrono-amperometric measurements of the electrospun materials as anodes showed a considerable decrease in start-up time and more than a tenfold increase in current generation using *S. oneidensis* MR-1 compared to conventional graphite electrode. The improved bioelectrocatalytic performance was mainly attributed to the increased specific surface area and porosity especially for blend materials. The fibrous and porous nature of these materials presumably provides the habitat for maximum growth of bacteria while permitting an efficient substrate supply and product exit.

Palladium (Pd)/carbon composite nanofibers with nanocactus- and nanoflower-like morphology (Fig. 8) were prepared by electrodepositing Pd onto surface of carbon nanofibers from electrospun PAN to act as a highly active catalyst toward the redox reactions of hydrogen peroxide

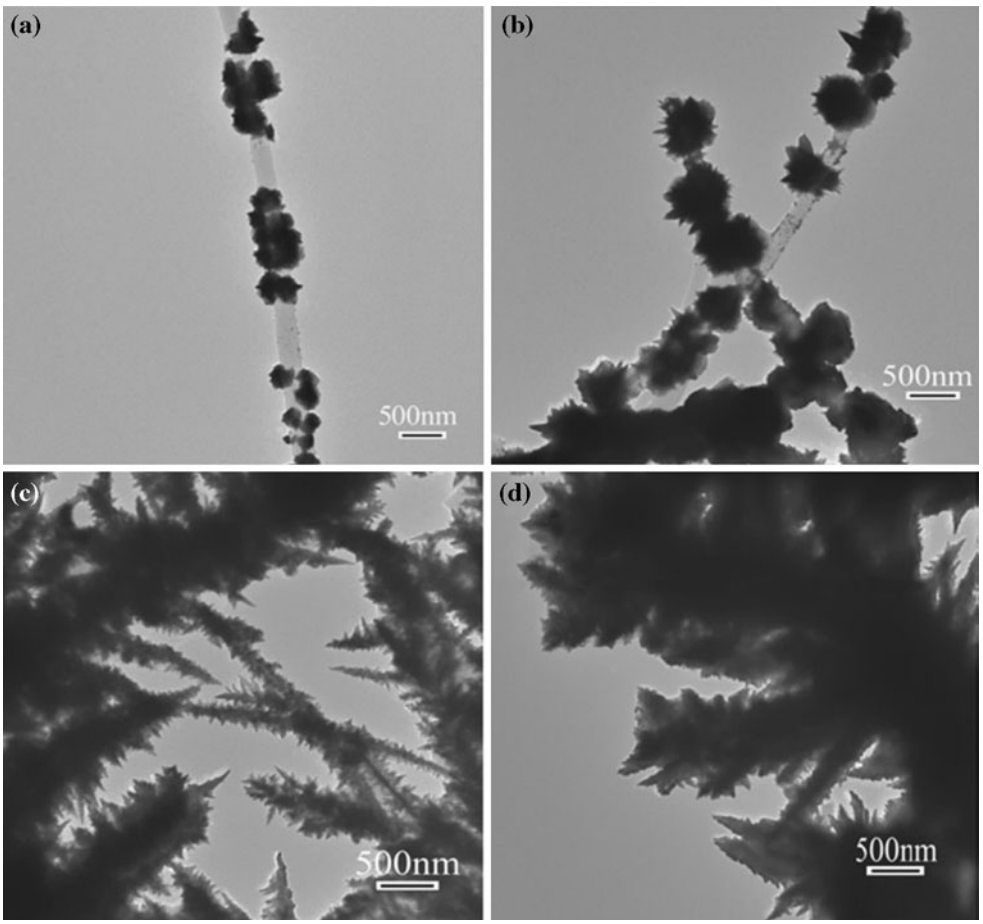

Fig. 8 TEM images of Pd/CNFs with different Pd deposition times: **a** 1.0; **b** 2.0; **c** 4.0; and **d** 8.0 h (deposition potential = −0.2 V) [81]

(H_2O_2) and β-nicotinamide adenine dinucleotide (β-NADH) [81]. Similar results are difficult to be acquired from spherical Pd nanoparticle-loaded carbon nanofibers. Another type of carbon composite nanofibers with homogeneously distributed Ag nanoparticles (AgNPs) on surface was fabricated by electrospinning and subsequent hydrothermal growth of AgNPs [82]. The carbon/AgNPs composite nanofibers showed high catalytic activity in reduction of 4-nitrophenol with $NaBH_4$ and the catalytic activity increased with the increase of silver content. This might be attributed to the high surface areas of AgNPs and synergistic effect on delivery of electrons between AgNPs and carbon nanofibers.

1D ZnO/carbon composite nanofibers (ZnO/CNFs) with high photocatalytic activity were successfully prepared by a simple combination of electrospinning and hydrothermal process to degrade organic pollutants under UV light irradiation [83]. It is demonstrated that carbon nanofibers from electrospun PAN with surface-coated ZnO exhibited higher photocatalytic property than pure ZnO for the degradation of Rhodamine B (RB, a test dye). The formation of heteroarchitectures might result in a cooperative or synergetic effect between CNFs and ZnO and an efficient separation of photo-generated electrons and holes was suggested. In later research, 1D heterostructures of Bi_2MoO_6/carbon nanofibers (Bi_2MoO_6-CNFs) [84] and In_2O_3/carbon nanofibers (In_2O_3-CNFs) [85] were prepared by combination of electrospinning technique and solvothermal process. Secondary Bi_2MoO_6 and In_2O_3 nanostructures were successfully grown on the primary CNF substrates and their morphology could be controlled by adjusting the solvothermal reaction parameters. Enhanced photocatalytic activity was observed for those heterostructures under visible light compared to pure Bi_2MoO_6 or In_2O_3. The enhancement could be attributed to the formation of heterostructures that might improve the separation of photo-generated electrons and holes. Furthermore the heterogeneous nanostructures could be easily recycled without impairing the photocatalytic activity.

Sensor

Sensors/detectors with simple construction, convenient operation, fast and stable response, high sensitivity, and

good selectivity are always desirable to meet the great demands for determination of various chemicals and biomolecules. Among various detection techniques, electrochemical method has attracted considerable interests due to its simplicity, low cost and sensitivity. Carbon materials have been employed in electroanalytical investigations because of their chemical inertness in most electrolyte solutions and relatively wide potential window [86]. As a new and interesting type of material in carbon materials family, carbon nanofibers from electrospun PAN have attracted much attention in the area of sensors and biosensors because of their remarkable characteristics as 1D nano-scale structure, functionalization ability, electrochemical property, mechanical flexibility, and biocompatibility. Moreover recent findings also indicated that the electrochemical activities of carbon nanofiber webs from electrospun PAN can be controlled via their density of electronic states, which is varied by their nanosized graphite concentration through manipulation of carbonization conditions [87].

Carbon nanofiber modified carbon paste electrode (CNF-CPE) was developed by casting water suspension of carbon nanofibers from electrospun PAN onto the surface of a CPE. Without further treatment, the CNF-CPE electrode was able to directly detect three amino acids: L-tryptophan (Trp), L-tyrosine (Tyr), and L-cysteine (Cys) using cyclic voltammetry and constant potential amperometric method [88]. The results showed that the CNF-CPE possessed excellent electrocatalytic activity and good analytical performance toward the oxidation of these three amino acids. The linear ranges of Trp, Tyr, and Cys were 0.1–119, 0.2–107, and 0.15–64 μM, respectively, with a detection limit of 0.1 μM for all three, which insured a trace amount determination. The modified electrode also demonstrated advantages of good reproducibility, stability, and selectivity. The additional merit of this electrode such as ease of construct, low cost, and no treatment before use renders it feasible to be applied in routine clinical determination. CNF-CPE was also used to construct an amperometric sensor device without any enzyme or medium to detect xanthine (Xa) [89], the first indicator of an abnormal purine profile in human being and an index for evaluating the freshness of fish. Incorporation of carbon nanofibers from electrospun PAN significantly improved the analytical performance of CPE and exhibited rapid response, good selectivity, and stability. The dynamic linear range of Xa detection was 0.03–21.19 μM with the detection limit as low as 20 nM. The system was effectively applied to estimate the freshness of fish and determine Xa in human urine. CNF-CPE was further used to construct simple and sensitive sensors to simultaneously and quantitatively detect dihydroxybenzene isomers including catechol (CC) and hydroquinone (HQ) [90]. Compared to bare CPE electrode, the CNF-CPE electrode demonstrated much higher electrocatalytic activity toward the oxidation of dihydroxybenzene isomers with significant peak current increase and potential difference decrease between the oxidation and reduction peaks, a result from large specific surface area of the carbon nanofibers and a large amount of edge-plane-like defective sites on fiber surface. The results of cyclic voltammetry and differential pulse voltammetry demonstrated that CC and HQ could be detected selectively and sensitively with detection limits of 0.2 and 0.4 μM, respectively, and a linear range of 1–200 μM in both cases in the presence of 50 μM isomer. The sensor was applied for simultaneous determination of CC and HQ in lake water with satisfactory results.

Carboxylic acid group functionalized carbon nanofibers (FCNF) were integrated with other nanostructures to make composite electrodes for biosensing [91, 92]. Carbon nanofibers from electrospun PAN were first functionalized with carboxylic acid groups through nitric acid treatment and then used to incorporate hydroxyapatite (HA) or Prussian blue (PB) to make FCNFs-HA or FCNFs-PB composite. The FCNFs-HA composite was coated on a polished Au electrode followed by immobilization of cytochrome *c* on the surface of FCNFs-HA/Au electrode. The resulting biosensor demonstrated a good electrocatalytic activity and fast response to H_2O_2. The catalytic current was linear to H_2O_2 concentration in the range of 2.0 μM to 8.7 mM with a detection limit of 0.3 μM. The FCNFs-PB composite was coated on a polished glassy carbon electrode (GCE) and the resulting PB-FCNF/GCE electrode showed good electrocatalysis toward the reduction of H_2O_2. A glucose biosensor was developed by immobilizing glucose oxidase (GOD) onto PB-FCNF/GCE electrode. The glucose biosensor exhibited a rapid response of 5 s, a low detection limit of 0.5 μM, a wide linear range of 0.02–12 mM, and a high sensitivity of 35.94 μA cm^{-2} mM^{-1} in addition to good stability, repeatability, and selectivity.

Not only pure carbon nanofibers but also metal nanoparticle-loaded carbon nanofibers could be used to modify electrodes. In one research, Pd nanoparticle-loaded carbon nanofibers (PdNPs/CNFs) were prepared by electrospinning PAN with palladium(II) acetate followed by thermal treatment and subsequently used to coat CPE [93]. The PdNPs/CNF-CPE electrode exhibited excellent electrochemical catalytic activities toward dopamine (DA), uric acid (UA), and ascorbic acid (AA), which three usually coexist in biological samples, by significantly decreasing their oxidation overpotentials and enhancing their peak currents. Therefore simultaneous determination of DA, UA, and AA in their ternary mixture was achieved using differential pulse voltammetry through Pd/CNF-CPE electrode. The lowest detection limits of DA, UA, and AA

were observed at 0.2, 0.7, 15 μM, respectively. Similarly rhodium nanoparticle-loaded carbon nanofibers (RhNPs/CNFs) were prepared by electrospinning PAN with rhodium acetate followed by carbonization [94]. The RhNPs/CNFs were dispersed in DMF under ultrasonic agitation and then cast on the surface of pretreated pyrolytic graphite electrode (PGE). The modified electrode demonstrated excellent electrocatalytic activity toward hydrazine oxidation and thus can be used for highly sensitive and selective sensing of hydrazine. In a more recent research, cobalt nanoparticles-decorated carbon nanofibers (CoNPs/CNFs) were synthesized by a two-step approach comprised of electrospinning of PAN and thermal treatment [95]. The CoNPs-CNFs nanocomposites modified GCE electrode showed a pH-controlled electrocatalytic activity toward the oxidation of cysteine and *N*-acetyl cysteine, which was used to fabricate an enzymeless sensor for amino acid.

Carbon nanofibers from electrospun PAN could also be used alone to make an electrode that was further loaded with Pt nanoparticles through the reduction reaction of H_2PtCl_6 at room temperature [96]. This PtNPs/CNFs composite electrode exhibited high sensitivity and good selectivity for amperometric detection of H_2O_2. The detection limit of 0.6 μM with a wide linear range of 1–800 μM was superior compared to what had been previously observed in other H_2O_2 electrochemical sensors. The PtNPs/CNFs electrode also showed good selectivity for H_2O_2 detection in the presence of AA, acetaminophenol, and UA.

In addition to electrochemical detection of chemicals, carbon nanofiber mats from electrospun PAN can detect gases through resistance change. Ultrafine carbon nanofibers decorated with ZnO/SnO_2 nanoparticles were fabricated through single-nozzle co-electrospinning technique that used a phase-separated polymer solution mixture containing PAN, PVP, zinc acetate, and tin chloride followed by a heat treatment up to 800 °C [97]. The metal precursors of zinc acetate and tin chloride were first incorporated in PVP solution, then mixed with PAN solution, and further converted to metal oxide after heat treatment. These hybrid carbon nanofibers were deposited on an interdigitated electrode array (IDA) and constructed to detect dimethyl methylphosphonate (DMMP), a simulant for the Sarin. The minimum detectable level was as low as 0.1 ppb (Fig. 9). In a recent research, carbon nanofibrous mat (nano-felt) surface-attached with Pd nanoparticles was prepared by successive multi-steps: (1) functionalization of the surface of electrospun PAN nanofibers with amidoxime groups; (2) chelation of Pd^{2+} on fiber surface; (3) Pd^{2+} reduction; and (4) PAN carbonization [98]. This material was mechanically flexible/resilient and showed excellent hydrogen sensing capability at room temperature. The amidoxime surface-functionalized PAN nano-felt could be a general precursor material to prepare carbon nano-felts surface-attached with different metal nanoparticles for a variety of applications. Pd nanoparticles could be alternatively deposited on carbon nanofiber surface via the supercritical CO_2 method for sensing of H_2 [99]. In this approach, Pd acetylacetonate was dissolved in supercritical CO_2/acetone and carried onto the surfaces of carbon nanofibers from electrospun PAN by supercritical CO_2. Following heat treatment at 600 °C converted the Pd precursor to Pd nanoparticles on carbon nanofiber surface. In another research, a sensitive NO and CO gas sensor based on carbon nanofibers from electrospun PAN was developed by a multiple-step preparation [100]: (1) integrate carbon black in carbon nanofibers through co-electrospinning of PAN and carbon black; (2) activate the carbon nanofibers through KOH treatment at high temperature; and (3) modify the surface of carbon nanofibers by fluorination. It was revealed that (1) carbon black additives increased the overall electrical conductivity and efficiently transferred resistive response from the surface of gas sensor to electrode; (2) KOH chemical activation resulted in a porous fiber structure with 100 times more specific surface area and thus significantly increased target gas adsorption; and (3) the induced functional groups from surface modification attracted target gas to the surface of gas sensor. The sensitivity of NO and CO gases was improved about five times through this multiple-step preparation.

Adsorption/separation

Economic and efficient adsorption media for high capacity and high throughput separation/adsorption are always in great demands with the development of science and technology. Carbon materials, particularly activated carbons, have been used as a powerful adsorbent for a long time [101, 102]. Carbon nanofiber membranes from electrospun PAN have quickly found their uses in the field of adsorption/separation due to their high specific surface area and large inter-fiber porosity. High specific surface area means more adsorption sites and high porosity implies smaller driving force to push the liquid media through the membrane, making the separation process more energy efficient.

Removal of disinfection byproducts (DBPs) from drinking water was attempted using carbon nanofiber membranes from electrospun PAN (CNMs) [103]. Chloroform and monochloroacetic acid (MCAA) were used as model DBPs compounds. Adsorption capacity of CNMs was higher than literature data of commercially available activated carbon and ACFs. The removal of DBPs from water was also investigated by using multiwalled carbon nanotubes (MWCNTs)-incorporated CNMs. The initial removal of MCAA was increased with increasing concentration of the MWCNTs, but subsequent removals

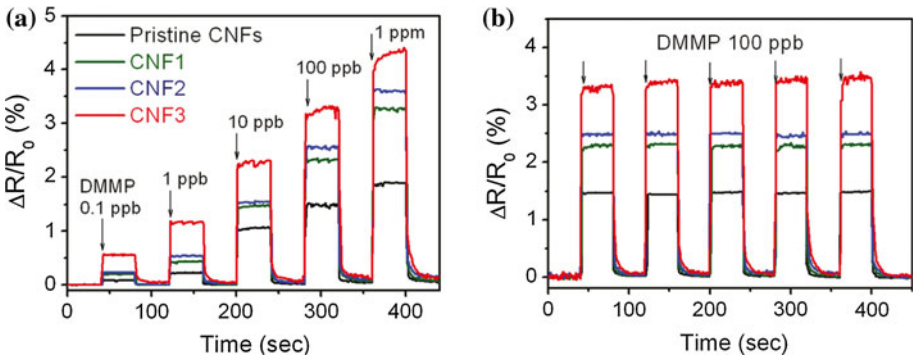

Fig. 9 Normalized resistance changes of carbon nanofibers decorated with ZnO/SnO_2 nanoparticles upon sequential exposure to various DMMP vapor concentrations (**a**) and periodic exposure to DMMP vapor of 100 ppb (**b**). Reversible and reproducible responses were measured at a constant current value (10^{-6} A) with amount and type of metal oxides on the CNF surfaces: *black* pristine CNFs, *green* CNF1 with 1 wt% ZnO, *blue* CNF2 with 1 wt% SnO_2, and *red* CNF3 with 1 wt% ZnO and SnO_2 [97] (Color figure online)

showed no effect of addition of MWCNTs. In another research, activated carbon nanofibers (ACNFs) were acquired by adding steam into inert gas flow during PAN nanofiber carbonization at 600 °C [104]. ACNFs with a variety of shallow and homogeneous microporous structures and nitrogen contents were attained by controlling carbonization and steam activation conditions. Compared to conventional thick ACFs, thin ACNFs were considered to possess more homogeneous and shallow pores (Fig. 10) and demonstrated superior capability for formaldehyde gas adsorption even at a low concentration and in a humid environment. ACNFs have also been employed as an effective tool to remove NO in polluted air [105]. Without any other catalyst, the ACNFs that were acquired by supplying 30 vol% steam into inert gas flow during carbonization of electrospun PAN nanofibers at 800 °C for 30 min exhibited high activities for NO removal at room temperature. Percentage of NO removed by 0.1 g of reported porous carbon nanofiber material was higher than 60 % when inlet NO concentration was 20 ppm. Under the same experimental condition, there was no outlet NO_x ($NO + NO_2$) could be detected within experimental duration when inlet NO concentration was 2 ppm.

Carbon nanofiber adsorption media have been demonstrated as a promising alternative to packed resin beds for bioseparation. The surface-functionalized carbon nanofibers from electrospun PAN with weak acid cation-exchange ligand were obtained by nitric acid treatment [106]. These carbon nanofiber mats were capable of adsorbing approximately ten-times more protein than their microfiber counterparts. Incorporation of a higher ligand density through prolonging functionalization time or by addition of a non-ionic surfactant to the adsorption environment resulted in more hydrophilic fiber surface that could minimize nonspecific adsorption from competing proteins and allow for more selective protein separation. Meanwhile, ultrafine fiber sizes (~300 nm) along with

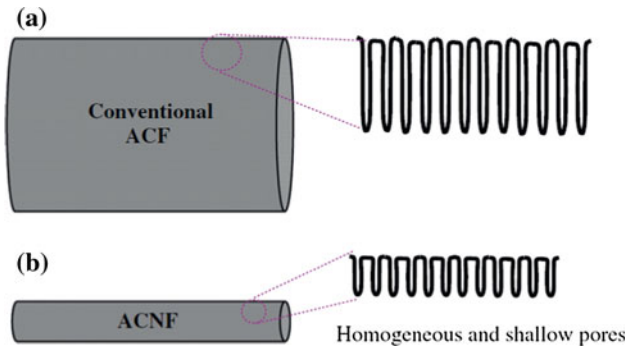

Fig. 10 Schematic diagram of pore structure of **a** conventional thick ACF and **b** thin ACNF [104]

inter-fiber open pores (~10–15 μm) in the carbon nanofiber mats led to higher operating flow rates and lower pressure drops.

Biomedical application

The application of carbon fibers in biomedical field has a history of more than 30 years up to date [107]. Based upon various clinical results, carbon fibers can be judged as a safe material for biomedical applications. With the development of nano-scaled carbon fibers from electrospun PAN, the biomedical applications of these novel carbon materials have attracted attention [108].

Carbon nanofibers containing β-tricalcium phosphate nanoparticles (β-TCP/CNFs) were produced by electrospinning PAN with triethyl phosphate and calcium nitrate tetrahydrate followed by stabilization at 260 °C and carbonization at 1100 °C [109]. The results from cell culture indicated that this material had good biocompatibility and was more favorable for cell growth as compared to pure carbon nanofibers. More importantly β-TCP improved the degradation properties of carbon nanofibers in physiological environment. β-TCP/CNFs were able to degraded into

short segments owing to the dissolution of β-TCP nanoparticles, which may be easily eliminated from systemic blood circulation through renal excretion route (Fig. 11).

Natural bone is a fiber-reinforced hybrid material composed of type-I collagen fibers and hydroxyapatite (HAP) minerals. Carbon nanofibers from electrospun PAN (CNFs) were used to prepare CNFs/HAP composite to mimic the collagen fiber/HAP composite structure in natural bone [110]. CNFs were activated first by introducing carboxylic groups through treatment in concentrated NaOH aqueous solutions and soaked in simulated body fluid at 37 °C for 1–72 h. HAP nanoparticles grew quickly on these fibers throughout the thickness of the carbon nanofiber mats. The results indicated that bioactive HAP strongly interacted with the CNFs through coordination bonds and would provide strong interfacial bonding to host tissues. Fracture strength of the CNFs/HAP composite reached 67.3 MPa with 41.3 % CNFs. The CNFs/HAP composite materials demonstrated bright prospect as load-bearing artificial bone materials.

Bioactive glass (BG) is a bioceramic that has been long investigated for applications in bone regeneration. Composite carbon nanofibers with BG (CNFs/BG) were developed as substrate for bone regeneration uses [111]. BG precursors including calcium nitrate, triethyl phosphate, and TEOS were mixed and hydrolyzed to form a sol–gel solution and subsequently added to DMF solution of PAN. The resulting mixture solution was electrospun to form PAN nanofibers containing BG precursors. Upon stabilization and carbonization, continuous carbon nanofibers embedded with BG nanoparticles were generated. Biomineralization in simulated body fluid and in vitro co-culture with MC3T3-E1 osteoblasts revealed improved ability of CNFs/BG composites to promote the in vitro formation of apatite and MC3T3-E1 proliferation when compared to pure CNFs.

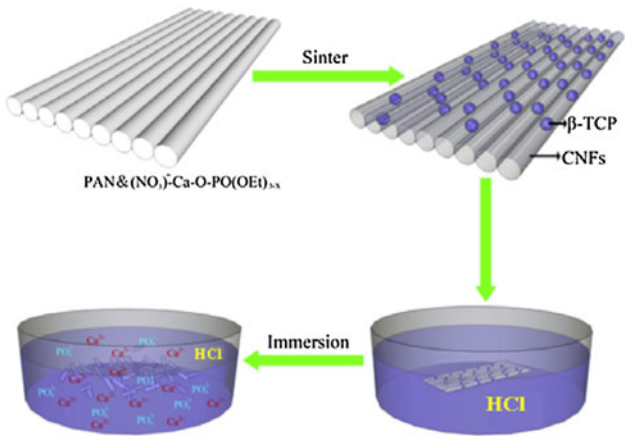

Fig. 11 Schematic diagram of the preparation of β-TCP/CNFs and CNF break-up [109]

High-strength carbon nanofibers

The theoretical tensile strength of carbon fibers is over 180 GPa [1, 2]. After many years of research, the strongest carbon fibers that can be produced today have a tensile strength of merely ~7 GPa (T1000®). Research has revealed that the mechanical strength of carbon fibers increases as the diameter of precursor fibers decreases when they are produced under comparable conditions, i.e., a smaller diameter allows a higher fraction of the theoretical strength to be achieved [112]. This is well-known as "size effect." Carbon fibers (T1000®) with an average diameter of ~5 μm and tensile strength of ~7 GPa have been produced by reducing the size of orifices in the spinneret from ~70 to ~40 μm. However, conventional spinning methods make it extremely difficult, if not impossible, to prepare precursor fibers with diameters that are orders of magnitude smaller than 10 μm. The facts that electrospinning makes significantly smaller fibers and electrospun nanofibers bear the potential of macromolecular orientation deserve every single effort to explore high-strength carbon fibers from electrospinning of PAN. Nonetheless, current endeavor toward high-strength carbon nanofibers is very limited due to the reality that carbon nanofibers from electrospun PAN do not possess high mechanical strength as they are expected [32] and methods and techniques to characterize single carbon nanofiber are still under development [113, 114].

A series of work has been done by Fong and co-workers to improve the mechanical properties of carbon nanofibers from electrospun PAN. Thermo-chemical reactions and the resulting structural conversions during the oxidative stabilization of electrospun PAN nanofibers have been systematically investigated and the results were compared with those of conventional PAN fibers made from wet spinning [115]. The findings are (1) PAN macromolecules in electrospun nanofibers predominantly underwent intermolecular cyclization and crosslinking during the early stages of stabilization while the conventional PAN fibers underwent intra-molecular cyclization; (2) the nitrile groups in the electrospun PAN nanofibers possessed a higher reactivity than those in conventional PAN fibers; and (3) the structural conversion from linear macromolecules to aromatic ring/ladder structures in the electrospun nanofibers occurred faster and more thoroughly under the same stabilization condition. Since stabilization is one essential process in carbon nanofiber formation, the findings from this research as well as a similar later research [116] laid solid foundation for developing high-strength carbon nanofibers from electrospun PAN nanofibers.

Apparently aligned nanofiber bundles outperform either single nanofiber or nonwoven nanofiber mat from the point of view of mechanical properties [117, 118]. Highly aligned

electrospun PAN nanofiber bundles were collected on the rim of a fast rotating disk [119]. The bundles were tightly wrapped onto a glass rod during oxidative stabilization in air and further carbonized in a temperature range from 1000 to 2200 °C. The research revealed that the average diameter of stabilized PAN nanofibers did not change while the average diameter of carbonized PAN nanofibers reduced significantly. With the increase of carbonization temperature, carbon nanofibers became more graphitic and structurally ordered. The mechanical properties of these carbon nanofiber bundles increased with the increase of carbonization temperature. The tensile strength of these carbon nanofiber bundles was in the ranges of 300–600 MPa and Young's moduli were in the ranges of 40–60 GPa. In a following study, 1–5 wt% phosphoric acid (PA) was included into electrospun PAN nanofibers as stabilization promoter [120]. The aligned electrospun PAN nanofiber bundles with PA were first stabilized in air at 230 °C, carbonized at 1000 °C, and graphitized in vacuum at 2200 °C for 2 h to develop GCNFs. PA was found to be able to effectively initiate the cyclization of PAN and induce aromatization during oxidative stabilization. The GCNFs made from electrospun PAN nanofibers containing 1.5 wt% of PA exhibited 62.3% higher mechanical strength than those made from the electrospun PAN nanofibers without PA.

From the point of view of developing high-strength fibers, as-electrospun PAN precursor nanofibers have to be stretched to make strong carbon nanofibers [36]. Post-spinning stretch of electrospun PAN nanofibers was thus attempted [121]. A bundle of highly aligned electrospun PAN nanofibers was stretched in an oven at ~100 °C, and a pan of boiling water was maintained during the stretching process. The stretched PAN nanofiber bundles with final lengths being 2, 3, and 4 times of original lengths were successfully acquired (Fig. 12). The investigation indicated that the macromolecules in the as-electrospun PAN nanofibers were loosely oriented along fiber axes and a small extent of stretch could effectively improve PAN macromolecular orientation and increase PAN crystallinity. Most of PAN macromolecules in crystalline phase of both as-electrospun and stretched PAN nanofibers possessed a zig-zag conformation instead of a helical conformation. The post-spinning stretch process substantially improved the tensile strength and Young's modulus of PAN nanofiber bundles by 333 and 413 %, respectively. This effort is one of the first successful attempts to stretch electrospun PAN nanofibers, despite the effectiveness of stretching and the precise strength measurement of individual nanofibers were upon further investigations. In a more recent report, a flowing water bath was developed to collect continuous bundles of loosely aligned electrospun PAN nanofibers and the acquired PAN nanofiber bundles were subsequently stretched in hot water up to four times of their original lengths [122]. In comparison with the commonly adopted

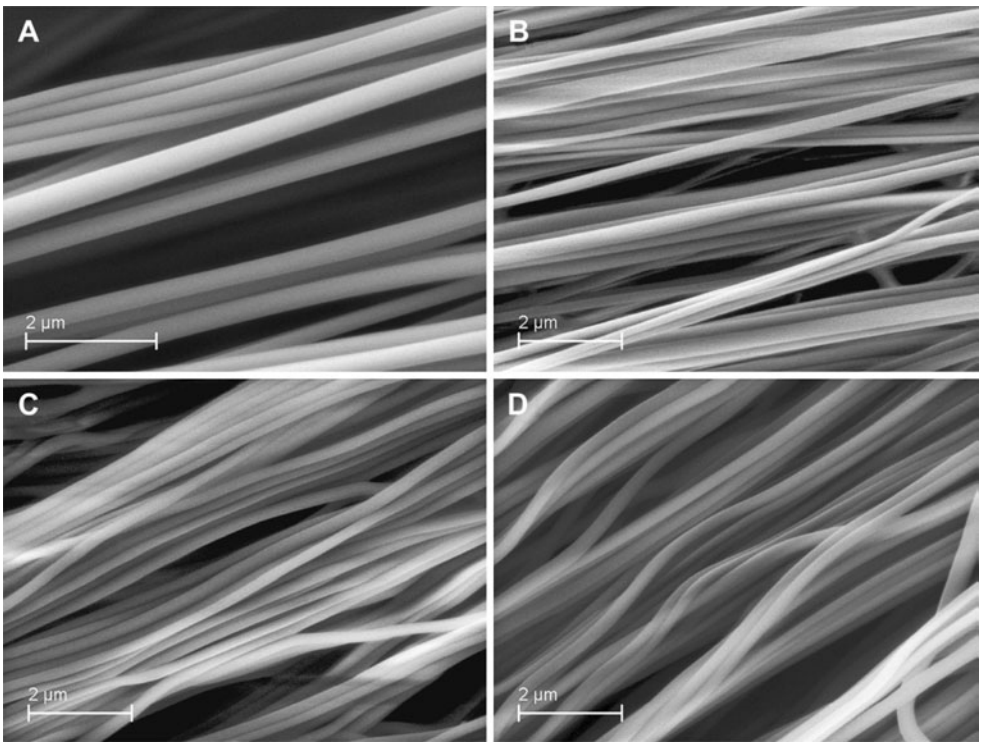

Fig. 12 SEM images showing representative morphologies of the as-electrospun PAN copolymer nanofiber bundle (**a**), the stretched nanofiber bundles with the final lengths being 2 (**b**), 3 (**c**), and 4 (**d**) times of original lengths [121]

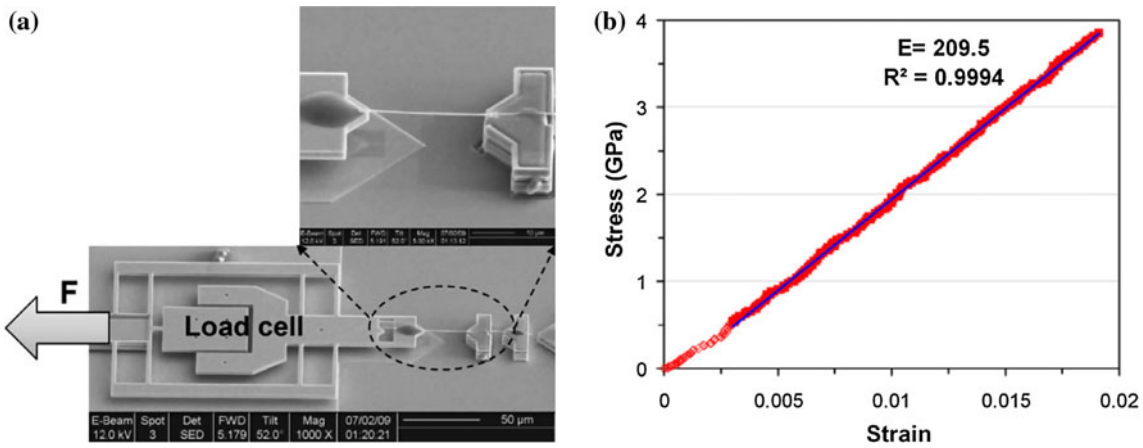

Fig. 13 SEM of a carbon nanofiber that mounted on a MEMS device showing detail of the specimen grips (**a**); engineering stress–strain curve from a single nanofiber carbonized at 1400 °C (**b**) [126]

nanofiber collection method such as rotating drum, the method of flowing water bath resulted in higher degree of uniaxial alignment in PAN nanofibers and more desired structural properties. The average fiber diameter of 4-time stretched PAN nanofiber bundles was reduced by 44 % of original value and the crystallinity and crystalline orientation degree of PAN were substantially improved by 72 and 100 %, respectively. The post-spinning stretch process also facilitated the stabilization of PAN. It is envisioned that the bundles of uniaxially aligned and post-spinning stretched electrospun PAN nanofibers would pave the road for the development of continuous nano-scaled carbon fibers with superior strength.

There are a few other researches in last 2 years that dealt with the mechanical properties of electrospun PAN nanofibers and carbon nanofibers derived therefrom. Aligned PAN nanofiber bundles and yarns were produced by two-nozzle conjugated electrospinning method and collected after fibers passed through a tubular electric heater [123] or were drawn in boiling water [124], respectively. In the former case, the stress and modulus of PAN nanofiber bundles with an average linear density of ~140 denier increased to 112.9 MPa and 7.25 GPa, respectively, after being treated at 270 °C in the tubular heater before collection on a rotating drum. In the latter case, the tensile strength of PAN nanofiber yarns increased to 350 MPa at draw ratio of 4. Moon and Farris studied the parameters of stabilization and carbonization of unidirectional yarns composed of electrospun PAN nanofibers including draw ratio, stabilization and carbonization temperature, heating rate, and exposure time [125]. The final carbon yarns derived from the electrospinning of 10 wt% PAN-DMF solution at 16 kV with 9.8 m s^{-1} take-up velocity had the highest ultimate strength of ~1 GPa by being stabilized from room temperature to 200 °C and being carbonized from room temperature to 1350 °C. A microelectromechanical (MEMS)-based testing platform with a high-resolution optics-based method for mechanical property experiment at nanoscale (Fig. 13) was developed to measure the mechanical property of individual PAN and carbon nanofiber [126]. High-strength carbon nanofibers had been acquired following process optimization in electrospinning, stabilization, and carbonization. The tensile strength and elastic modulus of individual nanofiber that was carbonized at 1400 °C had an average of 3.5 ± 0.6 and 172 ± 40 GPa, respectively, while the strength of some nanofibers reached over 4.5 GPa. The tensile strength and elastic modulus of these carbon nanofibers were six and three times larger than previously reported results, respectively.

Conclusions

From this review, it is evident that carbon nanofibers with hierarchical structures can be conveniently prepared by electrospinning PAN followed by stabilization and carbonization. This new class of carbon material with 1D nanostructure and concomitant high specific surface area has quickly found their applications in energy conversion and storage, catalysis, sensor, adsorption, and biomedical applications. Undoubtedly these carbon nanofibrous materials will be seen in many more applications across scientific and technological disciplines in the future. More intriguingly, strong carbon nanofibers have been attained through aligned electrospinning of PAN followed by post-spinning stretch and optimized stabilization and carbonization. The current attempts revealed a hope to acquire even stronger carbon fibers than those from conventional carbon fiber industry. Future research will be focused on the fundamental correlations between the processing conditions and the nanofiber structures. It is envisioned that the

continuous nano-scale carbon fibers from electrospun PAN are going to shine even greater luster in the family of carbon materials.

References

1. Rebouillat S, Peng JCM, Donnet J-B, Ryu S-K (1998) In: Donnet J-B, Wang TK, Rebouillat S, Peng JCM (eds) Carbon fibers, 3rd edn. Marcel Dekker, New York, pp 463–542
2. Morgan P (2005) Carbon fibers and their composites. CRC Press (Taylor & Francis Group), Boca Raton
3. Yusof N, Ismail AF (2012) J Anal Appl Pyrol 93:1
4. Wu J, Chung DDL (2002) Carbon 40:445
5. Rodriguez NM (1993) J Mater Res 8:3233
6. Tibbetts GG, Lake ML, Strong KL, Rice BP (2007) Compos Sci Technol 67:1709
7. Rahaman MSA, Ismail AF, Mustafa A (2007) Polym Degrad Stab 92:1421
8. Jong KPD, Geus JW (2000) Catal Rev: Sci Eng 42:481
9. Serp P, Corrias M, Kalck P (2003) Appl Catal A 253:337
10. Zou G, Zhang D, Dong C, Li H, Xiong K (2006) Carbon 44:828
11. Chun I, Reneker DH, Fong H, Fang X, Deitzel J, Beck Tan N, Kearns K (1999) J Adv Mater 31:36
12. Fong H, Reneker DH (2001) In: Salem DR (ed) Structure formation in polymeric fibers. Hanser Gardner Publications, Cincinnati, pp 225–246
13. Nataraj SK, Yang KS, Aminabhavi TM (2012) Prog Polym Sci 37:487
14. Inagaki M, Yang Y, Kang F (2012) Adv Mater 24:2547
15. Qin X-H, Wan Y-Q, He J-H, Zhang J, Yu J-Y, Wang S-Y (2004) Polymer 45:6409
16. Kalayci VE, Patra PK, Kim YK, Ugbolue SC, Warner SB (2005) Polymer 46:7191
17. Zhang L, Hsieh Y-L (2006) Nanotechnology 17:4416
18. Kirecci A, Ozkoc U, Icoglu HI (2012) J Appl Polym Sci 124:4961
19. Yarin AL, Koombhongse S, Reneker DH (2001) J Appl Phys 90:4836
20. Shin YM, Hohman MM, Brenner MP, Rutledge GC (2001) Polymer 42:9955
21. Reneker DH, Yarin AL, Fong H, Koombhongse S (2000) J Appl Phys 87:4531
22. Shin Y, Hohman M, Brenner M, Rutledge G (2001) Appl Phys Lett 78:1149
23. Hohman MM, Shin M, Rutledge G, Brenner MP (2001) Phys Fluids 13:2201
24. Zussman E, Rittel D, Yarin AL (2003) Appl Phys Lett 82:3958
25. Zhang H, Nie H, Yu D, Wu C, Zhang Y, White CJB, Zhu L (2010) Desalination 256:141
26. Zhang L, Luo J, Menkhaus TJ, Varadaraju H, Sun Y, Fong H (2011) J Membr Sci 369:499
27. Guo Z, Shao C, Mu J, Zhang M, Zhang Z, Zhang P, Chen B, Liu Y (2011) Catal Commun 12:880
28. Li Y, Quan J, Branford-White C, Williams GR, Wu J-X, Zhu L-M (2012) J Mol Catal B 76:15
29. Wang Y, Serrano S, Santiago-Aviles JJ (2003) Synth Met 138:423
30. Ko F, Gogotsi Y, Ali A, Naguib N, Ye H, Yang G, Li C, Willis P (2003) Adv Mater 15:1161
31. Hou H, Ge JJ, Zeng J, Li Q, Reneker DH, Greiner A, Cheng SZD (2005) Chem Mater 17:967
32. Zussman E, Chen X, Ding W, Calabri L, Dikin DA, Quintana JP, Ruoff RS (2005) Carbon 43:2175
33. Kim C, Yang KS, Kojima M, Yoshida K, Kim YJ, Kim YA, Endo M (2006) Adv Funct Mater 16:2393
34. Wu M, Wang Q, Li K, Wu Y, Liu H (2012) Polym Degrad Stab 97:1511
35. Zhang L, Hsieh Y-L (2009) Eur Polymer J 45:47
36. Liu J, Yue Z, Fong H (2009) Small 5:536
37. Liu C, Li F, Ma L-P, Cheng H-M (2010) Adv Mater 22:E28
38. Liu X-M, Huang ZD, Oh SW, Zhang B, Ma P-C, Yuen MMF, Kim J-K (2012) Compos Sci Technol 72:121
39. Candelaria SL, Shao Y, Zhou W, Li X, Xiao J, Zhang J-G, Wang Y, Liu J, Li J, Cao G (2012) Nano Energy 1:195
40. Hedin N, Sobolev V, Zhang L, Zhu Z, Fong H (2011) J Mater Sci 46:6453. doi:10.1007/s10853-011-5725-z
41. Kumar PS, Sahay R, Aravindan V, Sundaramurthy J, Ling WC, Thavasi V, Mhaisalkar SG, Madhavi S, Ramakrishna S (2012) J Phys D 45:265302
42. Ji L, Yao Y, Toprakci O, Lin Z, Liang Y, Shi Q, Medford AJ, Millns CR, Zhang X (2010) J Power Sources 195:2050
43. Chen Y, Lu Z, Zhou L, Mai Y-W, Huang H (2012) Nanoscale 4:6800
44. Li Y, Guo B, Ji L, Lin Z, Xu G, Liang Y, Zhang S, Toprakci O, Hu Y, Alcoutlabi M, Zhang X (2013) Carbon 51:185
45. Zhang W-J (2011) J Power Sources 196:13
46. Yu Y, Yang Q, Teng D, Yang X, Ryu S (2010) Electrochem Commun 12:1187
47. Bonino CA, Ji L, Lin Z, Toprakci O, Zhang X, Khan SA (2011) ACS Appl Mater Interfaces 3:2534
48. Kim D, Lee D, Kim J, Moon J (2012) ACS Appl Mater Interfaces 4:5408
49. Ji L, Lin Z, Alcoutlabi M, Toprakci O, Yao Y, Xu G, Li S, Zhang X (2012) RSC Adv 2:192
50. Wang B, Cheng J, Wu Y, Wang D, He D (2013) J Mater Chem A 1:1368
51. Yang Z, Du G, Meng Q, Guo Z, Yu X, Chen Z, Guo T, Zeng R (2012) J Mater Chem 22:5848
52. Ji L, Toprakci O, Alcoutlabi M, Yao Y, Li Y, Zhang S, Guo B, Lin Z, Zhang X (2012) ACS Appl Mater Interfaces 4:2672
53. Yang G, Li Y, Ji H, Wang H, Gao P, Wang L, Liu H, Pinto J, Jiang X (2012) J Power Source 216:353
54. Zhang S, Lin Z, Ji L, Li Y, Xu G, Xue L, Li S, Lu Y, Toprakci O, Zhang X (2012) J Mater Chem 22:14661
55. Zhang S, Li Y, Xu G, Li S, Lu Y, Toprakci O, Zhang X (2012) Source 213:10
56. Dimesso L, Spanheimer C, Jaegermann W, Zhang Y, Yarin AL (2012) J Appl Phys 111:064307
57. Toprakci O, Toprakci HAK, Ji L, Lin Z, Gu R, Zhang X (2012) J Renew Sustain Energy 4:013121
58. Zhang S, Lu Y, Xu G, Li Y, Zhang X (2012) J Phys D 45:395301
59. Kim B-H, Yang KS, Bang YH, Kim SR (2011) Mater Lett 65:3479
60. Kim B-H, Yang KS, Woo H-G (2011) Electrochem Commun 13:1042
61. Kim B-H, Yang KS, Woo H-G, Oshida K (2011) Synth Met 161:1211
62. Kim B-H, Kim CH, Yang KS, Rahy A, Yang DJ (2012) Electrochim Acta 83:335
63. Kim B-H, Yang KS, Woo H-G (2013) Mater Lett 93:190
64. Zhou Z, Wu X-F (2013) J Power Source 222:410
65. Kim B-H, Yang KS, Ferraris JP (2012) Electrochim Acta 75:325
66. Kim SY, Kim B-H, Yang KS, Oshida K (2012) Mater Lett 87:157
67. Niu H, Zhang J, Xie Z, Wang X, Lin T (2011) Carbon 49:2380

68. Jung K-H, Deng W, Smith DW Jr, Ferraris JP (2012) Electrochem Commun 23:149
69. Xie Y, Joshi P, Darling SB, Chen Q, Zhang T, Galipeau D, Qiao Q (2010) J Phys Chem C 114:17880
70. Hsieh C-T, Yang B-H, Lin J-Y (2011) Carbon 49:3092
71. Joshi P, Zhang L, Chen Q, Galipeau D, Fong H, Qiao Q (2010) ACS Appl Mater Interfaces 2:3572
72. Poudel P, Zhang L, Joshi P, Venkatesan S, Fong H, Qiao Q (2012) Nanoscale 4:4726
73. Park S-H, Jung H-R, Kim B-K, Lee W-J (2012) J Photochem Photobiol A 246:45
74. Che A-F, Germain V, Cretin M, Cornu D, Innocent C, Tingry S (2011) New J Chem 35:2848
75. Wang M-X, Huang Z-H, Shimohara T, Kang F, Liang K (2011) Chem Eng J 170:505
76. Wang M-X, Huang Z-H, Shen K, Kang F, Liang K (2013) Catal Today 201:109
77. Qiu Y, Yu J, Shi T, Zhou X, Bai X, Huang JY (2011) J Power Sources 196:9862
78. Yin J, Qiu Y, Yu J (2013) Electrochem Commun 30:1
79. Jeong B, Uhm S, Lee J (2010) ECS Trans 33:1757
80. Patil SA, Chigome S, Hagerhall C, Torto N, Gorton L (2013) Bioresour Technol 132:121
81. Lin Z, Ji L, Medford AJ, Shi Q, Krause WE, Zhang X (2011) J Solid State Electrochem 15:1287
82. Zhang P, Shao C, Zhang Z, Zhang M, Mu J, Guo Z, Liu Y (2011) Nanoscale 3:3357
83. Mu J, Shao C, Guo Z, Zhang Z, Zhang M, Zhang P, Chen B, Liu Y (2011) ACS Appl Mater Interfaces 3:590
84. Zhang M, Shao C, Mu J, Huang X, Zhang Z, Guo Z, Zhang P, Liu Y (2012) J Mater Chem 22:577
85. Mu J, Shao C, Guo Z, Zhang M, Zhang Z, Zhang P, Chen B, Liu Y (2012) J Mater Chem 22:1786
86. Huang J, Liu Y, You T (2010) Anal Methods 2:202
87. Mao X, Simeon F, Rutledge GC, Hatton TA (2013) Adv Mater 25:1309
88. Tang X, Liu Y, Hou H, You T (2010) Talanta 80:2182
89. Tang X, Liu Y, Hou H, You T (2011) Talanta 83:1410
90. Guo Q, Huang J, Chen P, Liu Y, Hou H, You T (2012) Sens Actuators B 163:179
91. Cui K, Song Y, Guo Q, Xu F, Zhang Y, Shi Y, Wang L, Hou H, Li Z (2011) Sens Actuators B 160:435
92. Wang L, Ye Y, Zhu H, Song Y, He S, Xu F, Hou H (2012) Nanotechnology 23:455502
93. Huang J, Liu Y, Hou H, You T (2008) Biosens Bioelectron 24:632
94. Hu G, Zhou Z, Guo Y, Hou H, Shao S (2010) Electrochem Commun 12:422
95. Song Y, He Z, Xu F, Hou H, Wang L (2012) Sens Actuators B 166–167:357
96. Liu Y, Wang D, Xu L, Hou H, You T (2011) Biosens Bioelectron 26:4585
97. Lee JS, Kwon OS, Park SJ, Park EU, You SA, Yoon H, Jang J (2011) ACS Nano 5:7992
98. Zhang L, Wang X, Zhao Y, Zhu Z, Fong H (2012) Mater Lett 68:133
99. Zhao Y, Wang X, Lai C, He G, Zhang L, Fong H, Zhu Z (2012) RSC Adv 2:10195
100. Im JS, Kang SC, Lee S-H, Lee Y-S (2010) Carbon 48:2573
101. Ismail AF, David LIB (2001) J Membr Sci 193:1
102. Dabrowski A, Podkoscielny P, Hubicki Z, Barczak M (2005) Chemosphere 58:1049
103. Singh G, Rana D, Matsuura T, Ramakrishna S, Narbaitz RM, Tabe S (2010) Sep Purif Technol 74:202
104. Lee KJ, Shiratori N, Lee GH, Miyawaki J, Mochida I, Yoo S-H, Jang J (2010) Carbon 48:4248
105. Wang M-X, Huang Z-H, Shimohara T, Kang F, Liang K (2011) Chem Eng J 170:505
106. Schneiderman S, Zhang L, Fong H, Menkhaus TJ (2011) J Chromatogr A 1218:8989
107. Saito N, Aoki K, Usui Y, Shimizu M, Hara K, Narita N, Ogihara N, Nakamura K, Ishigaki N, Kato H, Haniu H, Taruta S, Kim YA, Endo M (2011) Chem Soc Rev 40:3824
108. Cunha C, Panseri S, Antonini S (2011) Nanomed Nanotechnol Biol Med 7:50
109. Liu H, Cai Q, Liang P, Fang Z, Duan S, Ryu S, Yang X, Deng X (2010) Carbon 48:2266
110. Wu M, Wang Q, Liu X, Liu H (2013) Carbon 51:335
111. Yang Q, Sui G, Shi YZ, Duan S, Bao JQ, Cai Q, Yang XP (2013) Carbon 56:288
112. Fitzer E (1989) Carbon 27:621
113. Tan EPS, Lim CT (2006) Compos Sci Technol 66:1102
114. Zhang J, Loya P, Peng C, Khabashesku V, Lou J (2012) Adv Funct Mater 22:4070
115. Liu J, Zhou P, Zhang L, Ma Z, Liang J, Fong H (2009) Carbon 47:1087
116. Wu M, Wang Q, Li K, Wu Y, Liu H (2012) Polym Degrad Stab 97:1511
117. Teo WE, Ramkrishna S (2006) Nanotechnology 17:R89
118. Teo WE, Inai R, Ramakrishna S (2011) Sci Technol Adv Mater 12:013002
119. Zhou Z, Lai C, Zhang L, Qian Y, Hou H, Reneker DH, Fong H (2009) Polymer 50:2999
120. Zhou Z, Liu K, Lai C, Zhang L, Li J, Hou H, Reneker DH, Fong H (2010) Polymer 51:2360
121. Lai C, Zhong G, Yue Z, Chen G, Zhang L, Vakili A, Wang Y, Zhu L, Liu J, Fong H (2011) Polymer 52:519
122. Liu J, Chen G, Gao H, Zhang L, Ma S, Liang J, Fong H (2012) Carbon 50:1262
123. Hosseini Ravandi SA, Sadrjahani M (2012) J Appl Polym Sci 124:3529
124. Hosseini Ravandi SA, Hassanabadi E, Tavanai H, Abuzade RA (2012) J Appl Polym Sci 124:5002
125. Moon SC, Farris RJ (2009) Carbon 47:2829
126. Arshad SN, Naraghi M, Chasiotis I (2011) Carbon 49:1710